Variable Sampling Composite Observer Based Frequency Locked Loop and its Application in Grid Connected System

Kulasekarapandian ARUN, Kamakshy SELVAJYOTHI
Faculty of Electronics Engineering, Indian Institute of Information Technology Design and Manufacturing Kancheepuram, Chennai 600127, India
ksjyothi@iiitdm.ac.in

***Abstract*—A modified digital signal processing procedure is described for the on-line estimation of DC, fundamental and harmonics of periodic signal. A frequency locked loop (FLL) incorporated within the parallel structure of observers is proposed to accommodate a wide range of frequency drift. The error in frequency generated under drifting frequencies has been used for changing the sampling frequency of the composite observer, so that the number of samples per cycle of the periodic waveform remains constant. A standard coupled oscillator with automatic gain control is used as numerically controlled oscillator (NCO) to generate the enabling pulses for the digital observer. The NCO gives an integer multiple of the fundamental frequency making it suitable for power quality applications. Another observer with DC and second harmonic blocks in the feedback path act as filter and reduces the double frequency content. A systematic study of the FLL is done and a method has been proposed to design the controller. The performance of FLL is validated through simulation and experimental studies. To illustrate applications of the new FLL, estimation of individual harmonics from nonlinear load and the design of a variable sampling resonant controller, for a single phase grid-connected inverter have been presented.**

***Index Terms*—discrete time systems, frequency locked loops, harmonic distortion, inverters, observers, power system harmonics, resonant controllers, state estimation.**

I. INTRODUCTION

Synchronization of power converter systems such as distributed renewable energy system, active filter, dynamic voltage restorer etc. with the grid requires accurate estimation of phase, frequency and magnitude even under distorted conditions. Phase locked loops (PLL) are widely used in extracting the grid information [1]. In single phase systems two types of phase detectors are used viz., the product type and Park transformation type. Product type PLL suffers from double frequency error. In [2] a modified product type detector, which eliminates the double frequency error, is discussed. In single phase systems the quadrature components are not available naturally and hence the direct use of synchronous reference frame (SRF) PLL as in three phase systems is not possible. In Park transformation type phase detector, quadrature component is artificially generated by transport delay [3], sliding discrete Fourier transform (SDFT) [4], inverse Park [3], [5], Hilbert transformation [5], second order generalized integrator (SOGI) [6-7], Kalman filter [8] etc. It has been found that the enhanced PLL (EPLL) reported in the literature is equivalent to SRF-PLL [9-14]. All these PLLs are based on constant sampling period.

Under polluted grid conditions, the in loop filter and pre-filter are used to minimize the effect of harmonics and DC offset in PLL. The product type [15], SDFT type [16] and cascaded delayed signal cancellation (CDSC) type [17] PLLs based on variable sampling rate had been employed in power applications. In addition to PLLs, FLLs are also reported for single phase system. Adaptive notch filter schemes [18-20], multiresonant frequency locked loop [21], [22] and composite observer [23], have been used to estimate grid parameters along with individual harmonics for time-varying signals. Main advantage of FLL is that the transient response is better during phase changes compared to PLL.

For power quality studies the variable sampling schemes are much suitable for keeping the number of samples (N) per cycle a constant. Variable sampling schemes are suitable for certain control applications such as repetitive control [24-25]. In this paper the concept of variable sampling composite observer based frequency locked loop is introduced. In variable sampling schemes [15-16], sampling pulses are generated by dividing the hardware clock which limits the number of samples per cycle. Power quality standard can be met either by reducing the number of samples per cycle or by choosing hardware with higher clock frequency. In [17], another method of generating the sampling pulses using NCO to make it independent of hardware clock is discussed.

In this proposal, the composite observer has been made adaptive to drifting frequency by varying the sampling period with the help of NCO. Variable sampling scheme eliminates the trigonometric computation in the observer blocks. NCO is derived from a standard coupled oscillator with automatic gain control described in [26]. Whatever might be the frequency of the input signal, the NCO provides constant number of samples per fundamental period. If the number of samples over a cycle is constant, digital signal processing of signals will be straight forward. It also lends itself for digital power quality measurements.

To filter out the double frequency components yielded by the product type phase detector, another composite observer (comprising the DC and second harmonic blocks) is incorporated in the frequency loop.

Organization of the paper is as follows: Section II introduces the concept of discrete time simple and

Digital Object Identifier 10.4316/AECE.2016.02005

composite observers. Proposed variable sampling FLL using composite observer is elaborated in section III. The design of integral controller for the proposed FLL is explained in section IV. Performance of the FLL scheme is discussed in section V. Section VI A, describes the estimation of individual harmonics from nonlinear load current. The design and implementation of variable sampling resonant controller proposed for grid connected inverter is dealt in section VI B.

II. Discrete Time Composite Observer

The fundamental block of an observer is derived from recursive discrete time sinusoidal oscillator. Any periodic sinusoidal signal can be modeled as the output of the sinusoidal oscillator. State space model of the digital wave-guide oscillator [26] is given as follows:

$$\begin{bmatrix} x_{11}((k+1)T) \\ x_{12}((k+1)T) \end{bmatrix} = \begin{bmatrix} \cos(\omega T) & \cos(\omega T)-1 \\ \cos(\omega T)+1 & \cos(\omega T) \end{bmatrix} \begin{bmatrix} x_{11}(kT) \\ x_{12}(kT) \end{bmatrix} \quad (1)$$

The output equation of the oscillator is given by:

$$y(kT) = x_{11}(kT) \quad (2)$$

The state space model and output equation of the discrete time observer [23] is described as follows:

$$\begin{bmatrix} \hat{x}_{11}((k+1)T) \\ \hat{x}_{12}((k+1)T) \end{bmatrix} = \begin{bmatrix} \cos(\omega T) & \cos(\omega T)-1 \\ \cos(\omega T)+1 & \cos(\omega T) \end{bmatrix} \begin{bmatrix} \hat{x}_{11}(kT) \\ \hat{x}_{12}(kT) \end{bmatrix} + \begin{bmatrix} L_1 e \\ L_2 e \end{bmatrix} \quad (3)$$

$$\hat{y}(kT) = \hat{x}_{11}(kT) \quad (4)$$

Structure of simple observer in discrete time is shown in Fig. 1. From (1), (2), (3) and (4) the characteristic equation of the observer can be derived as:

$$z^2 + (L_1 - 2\cos(\omega T))z + (L_2 - L_1)\cos(\omega T) + (1 - L_2) = 0 \quad (5)$$

In wave-guide oscillator structure, magnitude of the quadrature signal is made equal to that of the in-phase signal by multiplying the quadrature component with a gain factor $g_1 = \frac{(\cos(\omega T)-1)}{\sin(\omega T)}$ as shown in Fig. 1. For example, when ω = 2π × 50 for a sampling period of 0.02/512, $g_1 = \frac{\cos(2\pi/512)-1}{\sin(2\pi/512)} = -0.006136$. The observer gains ($L_1$, L_2) are calculated using pole placement technique.

The desired eigenvalues of observer matrix are chosen such that:

$$z = e^{-a\omega T}[\cos(\omega T) \pm j\sin(\omega T)] \quad (6)$$

The desired characteristic equation is given by:

$$z^2 - 2e^{-a\omega T}\cos(\omega T)z + e^{-2a\omega T} = 0 \quad (7)$$

The value of '*a*' decides the closed loop pole location of the observer in *z*-plane.

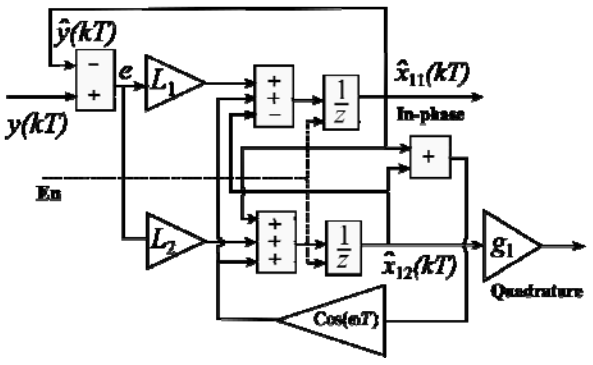

Figure 1. Structure of discrete time observer.

Gains (L_1, L_2) are calculated by comparing the coefficients of observer characteristic equation in (5) with that of the desired characteristic equation in (7).

The closed loop transfer function of the discrete time observer is:

$$\frac{\hat{y}(kT)}{y(kT)} = \frac{L_1 z - \cos(\omega T)L_1 + L_2\cos(\omega T) - L_2}{z^2 + (L_1 - 2\cos(\omega T))z + ((L_2 - L_1)\cos(\omega T) + (1 - L_2))} \quad (8)$$

The frequency response of the observer shown in Fig. 2 reveals that as the poles move closer to the unit circle the bandwidth gets reduced and the estimation time increases as illustrated in Fig. 3 for two different values of *a*.

The parallel structure of such blocks help to place the poles of observer inside the unit circle in such a way that all the harmonics are estimated at the same specified speed. In order to estimate the harmonic contents at the same instant as that of the fundamental, the harmonic component oscillator blocks are arranged in parallel along with the fundamental block as shown in Fig. 4 and assigned equi-dominant poles. The individual harmonics estimated by the composite parallel structure observer having DC, fundamental, third, fifth…up to the fifteenth harmonic blocks is illustrated in Fig. 5.

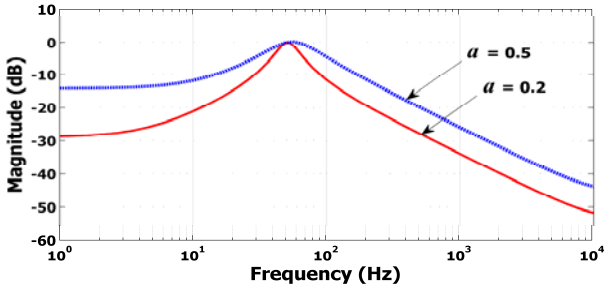

Figure 2. Magnitude plot of the discrete time observer designed for 50 Hz for pole locations corresponding to *a* = 0.2 and 0.5.

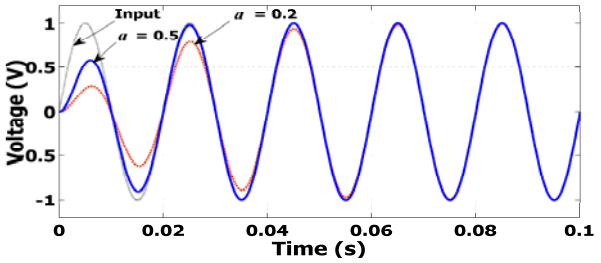

Figure 3. Output signal from a 50 Hz observer along with input signal for pole locations corresponding to *a* = 0.2 and 0.5.

The state space model of parallel structure of observer [23] having '*n*' blocks is given by:

$$\hat{x}((k+1)T) = A\hat{x}(kT) + Le(kT);\ \hat{y}(kT) = C\hat{x}(kT) \quad (9)$$

$$\text{where } A = \begin{bmatrix} 1 & 0 & 0 & .. & .. & 0 & 0 \\ 0 & \alpha_1 & (\alpha_1-1) & .. & .. & 0 & 0 \\ 0 & (\alpha_1+1) & \alpha_1 & .. & .. & 0 & 0 \\ : & : & : & : & : & : & : \\ 0 & 0 & 0 & .. & .. & \alpha_{m-1} & (\alpha_m-1) \\ 0 & 0 & 0 & .. & .. & (\alpha_m+1) & \alpha_m \end{bmatrix}$$

$$C = \begin{bmatrix} 1 & 1 & 0 & .. & .. & 1 & 0 \end{bmatrix},$$

$$L = \begin{bmatrix} L_0 & L_{11} & L_{12} & .. & .. & L_{m1} & L_{m2} \end{bmatrix},$$

$$\hat{x} = \begin{bmatrix} \hat{x}_0 & \hat{x}_{11} & \hat{x}_{12} & .. & .. & \hat{x}_{m1} & \hat{x}_{m2} \end{bmatrix} and$$

$$\alpha_n = \cos(n\omega T), n = 0,1,3...m,\ T = \frac{0.02}{512}.$$

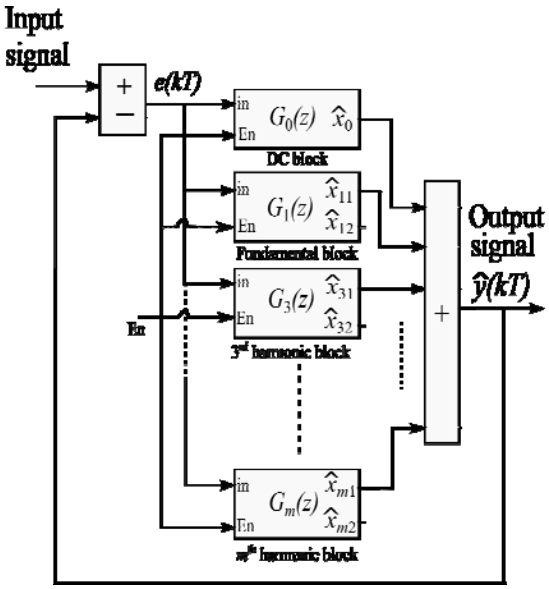

Figure 4. Parallel structure observer.

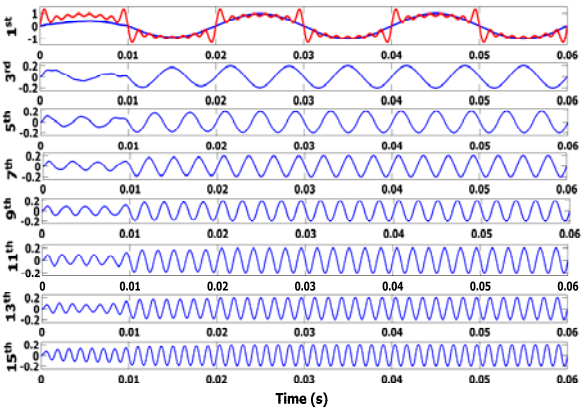

Figure 5. Estimated fundamental, third…up to the 15th harmonic along with the input signal for a 50 Hz composite parallel observer.

To get equal magnitude orthogonal components, the quadrature component of the fundamental has to be multiplied with g_1 as discussed in section II. In power systems, odd harmonic components are predominantly present and hence only DC and odd harmonic blocks are considered in the parallel structure observer.

The open loop transfer function of the n^{th} block is given by:

$$G_n(z) = \frac{L_{n1}z - \alpha_n L_{n1} + L_{n2}\alpha_n - L_{n2}}{z^2 - 2\alpha_n z + 1} \tag{10}$$

The closed loop characteristic equation of the parallel structure observer is:

$$G(z) = 1 + G_0(z) + G_1(z) + G_3(z) + ... + G_n(z) \tag{11}$$

The desired pole location for the system is chosen as follows:

$$z = e^{-a\omega T}(\alpha_n \pm j\beta_n) \quad \text{for } n = 0,1,3,5.....m \tag{12}$$

$$\text{where } \alpha_n = \cos(n\omega T), \beta_n = \sin(n\omega T)$$

The closed loop transfer of the fundamental component is given by:

$$Y_1(z) = \frac{G_1(z)}{1 + G_0(z) + G_1(z) + G_3(z).... + G_n(z)} \tag{13}$$

From (13), the magnitude response of the fundamental block of the parallel structure observer designed for 50 Hz with two different pole locations a = 0.2 and 0.5 are shown in Fig. 6 (a) and Fig. 6 (b) respectively.

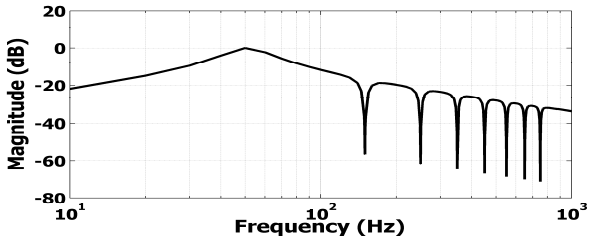

Figure 6(a). Magnitude plot for the fundamental block of composite observer with pole corresponding to $a = 0.2$.

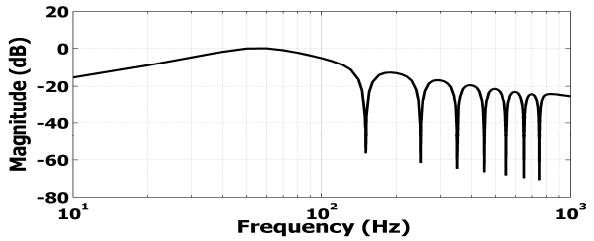

Figure 6(b). Magnitude plot for the fundamental block of composite observer with pole corresponding to $a = 0.5$.

The magnitude response shows that the fundamental block in the parallel structure accepts the fundamental frequency and rejects all other harmonics.

When there is a frequency drift in the input signal the estimated output from the observer has error in magnitude and phase. This necessitates frequency correction, which is explained in the following section.

III. Proposed Frequency Correction

The major issue is the wandering of frequency in power system from the central value, even if it remains within limits ± Δω. The observer structure consists of trigonometric term cos (ω*T*). When there is drift in frequency it requires computation of cos (ω + Δω)*T*. In the parallel structure of observer this trigonometric computation happens in '*m*' number of blocks. To eliminate the computation of cosine term of the observer, '*N*' is kept constant by varying the sampling frequency.

$$\omega T = (\omega \pm \Delta\omega)(T \mp \Delta T) = \frac{2\pi}{N} \tag{14}$$

where, *N* number of samples per cycle.

The proposed frequency correction is as shown in Fig. 7. In this scheme the phase error *p*(*kT*) is calculated from the product of the error *e*(*kT*) and the fundamental quadrature component (g_1) of the input signal.

$$p(kT) = e(kT).g_1 .\hat{x}_{12}(kT) \tag{15}$$

When there is a change in magnitude of the input signal, the performance of the FLL is affected. For reduced amplitude of the input signal, the frequency loop shows sluggish behavior and for an increase in amplitude, the frequency loop becomes oscillatory. To reduce these effects on frequency loop with respect to change in magnitude of the input signal, the phase error is normalized with a factor $\frac{1}{\hat{x}_{11}(kT)^2 + (g_1.\,\hat{x}_{12}(kT))^2}$.

This phase error contains DC and even harmonic components. An even harmonics (*m* = 0 and 2) composite observer is introduced in the feedback path to estimate the

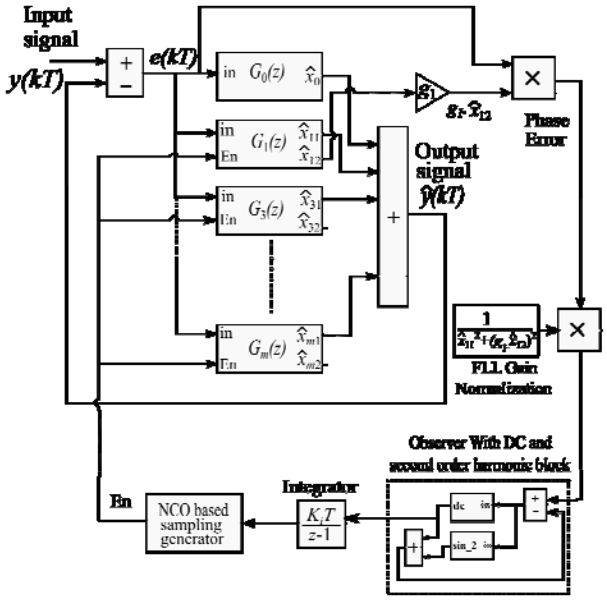

Figure 7. Proposed FLL using variable sampling period discrete composite observer.

DC component which is fed to an integrator for sampling frequency correction. The composite observer for estimating DC component has even order harmonic blocks, if the input signal contains only odd harmonic components. The pole locations of both the observers decide the settling time and bandwidth. The pole locations chosen deep inside the unit circle will give faster response for the system. The phase error is filtered and then integrated to get the frequency information.

In order to periodically trigger the computations in the observer blocks this frequency information from integrator is converted into pulses, which is done by the NCO. Thus in this proposal number of samples per cycle is kept as a constant at 512 for any frequency of the input signal. The sampling frequency is derived from the numerically controlled oscillator, which made the composite observer adaptable to drift in frequency condition.

A. Numerically Controlled Oscillator

The required enabling pulses for the observer are generated by using the standard coupled oscillator with automatic gain control given in [26] as:

$$\begin{bmatrix} x_1((k+1)T_o) \\ x_2((k+1)T_o) \end{bmatrix} = G_{NCO} \begin{bmatrix} 1-\frac{\beta_o^2}{2} & \beta_o \\ -\beta_o & 1-\frac{\beta_o^2}{2} \end{bmatrix} \begin{bmatrix} x_1(kT_o) \\ x_2(kT_o) \end{bmatrix} \quad (16)$$

where,

$$G_{NCO} = 3/2 - (x_1^2(kT_o) + x_2^2(kT_o)) \quad (17)$$

$$\beta_o = \sin(\omega_o T_o) \quad (18)$$

$$\omega_o = 2\pi f_o,\ T_o = \frac{1}{f_{NCO}}$$

Oscillator output frequency, $f_o = N f$,

f is input signal frequency $= 50$ Hz;

N is number of samples/cycle $= 512$,

NCO enabling frequency $f_{NCO} = 5$ MHz,

x_1 and x_2 are the state variables.

When the input frequency ω changes to ω + Δω, the output frequency ω_o of the oscillator changes to $\omega_o + \Delta\omega_o$. As the oscillator requires sinusoidal input, the input to the oscillator is given by:

$$\text{i.e., } \beta_o + \Delta\beta_o = \sin((\omega_o + \Delta\omega_o)T_o) \quad (19)$$

$$\Delta\beta_o = \sin(\omega_o T_o)\cos(\Delta\omega_o T_o) + \cos(\omega_o T_o)\sin(\Delta\omega_o T_o) - \beta_o \quad (20)$$

$\Delta\beta_o$ is plotted for change in frequency ranging ±20 Hz and is found to be linear as shown in Fig. 8.

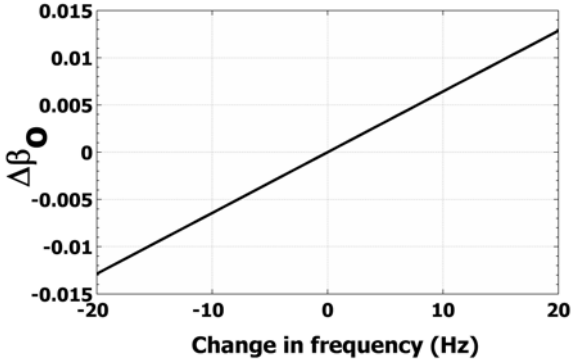

Figure 8. Variation of $\Delta\beta_o$ with respect to change in value of frequency.

Fig. 9 describes the generation of sampling pulses by use of NCO to get constant number of samples/cycle [17]. Here these samples are used to enable the composite observer. In this scheme, the output from the integral controller is approximately $\Delta\omega T$ and the oscillator requires $\beta_o + \Delta\beta_o$. Hence, a correction factor (K_{cor}) is to be incorporated and is calculated as follows:

$$\text{As } \Delta\omega_o T_o \to 0, \cos(\Delta\omega_o T_o) \to 1 \text{ and } \sin(\Delta\omega_o T_o) \to \Delta\omega_o T_o \quad (21)$$

Hence, (20) becomes

$$\Delta\beta_o \approx \Delta\omega_o T_o.\cos(\omega_o T_o) \approx (\Delta\omega T)(\frac{N}{T})(T_o)(\cos(\omega_o T_o)) \quad (22)$$

$$\Delta\beta_o \approx K_{cor}(\Delta\omega T) \quad (23)$$

From (22), the correction factor is obtained as:

$$K_{cor} = (\frac{NT_o}{T})(\cos(\omega_o T_o)) \quad (24)$$

Also, the inverse sine function of $\beta_o + \Delta\beta_o$ is taken to get the actual frequency. Only first two terms as described by (25) of inverse sine series is considered for this study and this provides frequency information with an accuracy of ±0.00002 Hz for a frequency range of 40 Hz to 70 Hz.

$$f + \Delta f = \frac{1}{2\pi N T_o}(\beta_o + \Delta\beta_o + \frac{(\beta_o + \Delta\beta_o)^3}{6}) \quad (25)$$

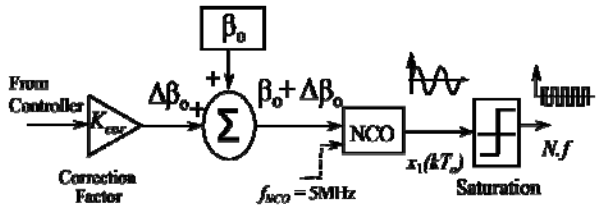

Figure 9. NCO based sampling generation for variable sampling FLL [17].

B. Step Change in frequency with and without filter

The transient behavior for sudden change in frequency of the FLL with even harmonics composite observer as a filter in feedback is studied with poles located on a circle of

radius $z = e^{-a_f \omega T}$, where (-a_f ω) real part of pole in *s*-domain, with a_f = 1. This observer contains DC and second harmonic blocks. The frequency of the input signal having THD 52.9 % is changed suddenly from 52.5 Hz to 47.5 Hz at *t* = 0.2 s. The response of composite observer is found to be smoother compared to that without filter as shown in Fig. 10.

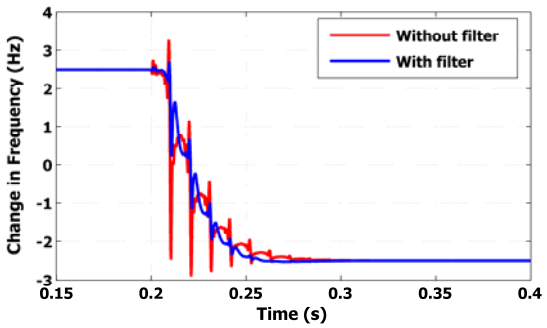

Figure 10. Transient response of FLL with and without feedback filter for step change in frequency from 52.5 Hz to 47.5 Hz.

IV. Design Of Integral Controller For FLL

The average value of phase error is positive for frequencies higher than the designed frequency and is negative for frequencies lower than the designed frequency. The NCO generates *N* times the input signal frequency. When the input signal frequency is changed by ±Δω the output of the NCO also gets changed to ±*N*.Δω. Hence, the integrator gain must be positive.

The performance of the FLL depends on three parameters such as the observer pole location, filter pole location and gain of the integrator. Equation (3) shows the nonlinear behavior of the system under drift in frequency. For tuning the controller, a linear continuous model is deduced and validated through simulation.

The observer is modeled as a first order system with a time constant t_{obs}. The discrete time observer with poles at *z* = $e^{-a\omega T}$ is equivalent to *s*-domain poles at *s* = -*a*ω. The continuous time model of the composite observer is obtained as $\frac{1}{1+st_{obs}}$, where $t_{obs} = \frac{1}{a\omega}$. Similarly, the transfer function of the even order composite observer based filter is $\frac{1}{1+st_f}$, where $t_f = \frac{1}{(a_f)\omega}$. The transfer function model of the scheme is shown in Fig. 11. The open loop transfer function of the scheme is:

$$G_{open} = \frac{K_{open} K_i}{s(1+st_{obs})(1+st_f)} \quad (26)$$

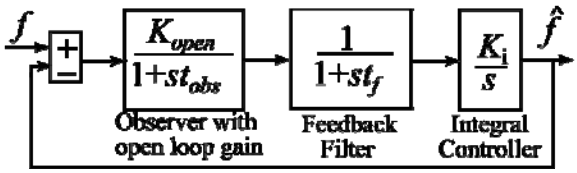

Figure 11. Transfer function model of the FLL.

The design of controller for the FLL is concerned with calculating the values of gains K_{open} and K_i. To calculate the open loop gain of the system (K_{open}), the integrator gain is kept unity (K_i = 1) with frequency loop open as shown in Fig. 12 for the actual system. The poles of the feedback observer (filter) is located with a_f = 1. With an input signal of unity magnitude for ±1 Hz, the slope is calculated from the change in integrator output vs time, as shown in Fig. 13. The absolute value of slope gives the system gain as:

$$K_{open} = \frac{|\Delta y|}{|\Delta x|} \quad (27)$$

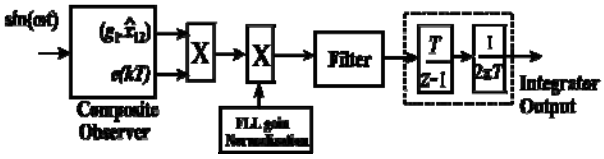

Figure 12. Block diagram for calculating the open loop gain of the system.

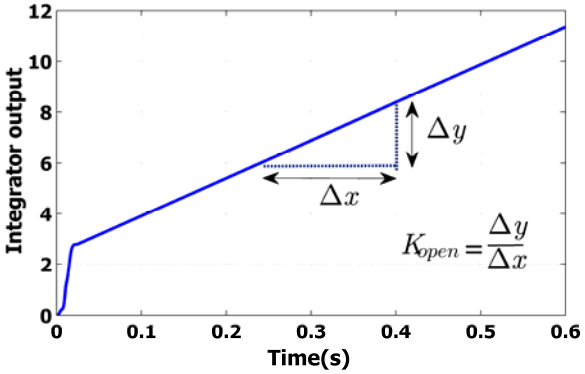

Figure 13. Integrator output vs time in open loop condition corresponding to pole location '*a* = 1'.

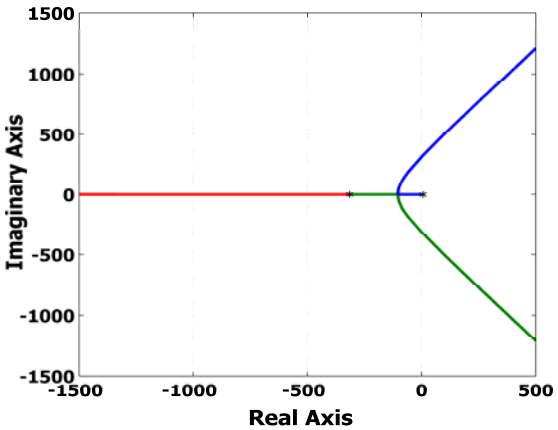

Figure 14. Root locus to find the integrator gain with pole location corresponding to '*a* = 1'.

The value of integrator gain (K_i) is obtained by plotting the root locus for the open loop system described in (26). The root locus of the system for t_{obs} = (1/ω) is shown in Fig. 14. The values of the system gain and the integrator gain for different pole locations and damping factors are shown in Table I.

TABLE I. SYSTEM GAIN AND INTEGRAL GAIN FOR VARIOUS DAMPING FACTOR WITH DIFFERENT POLE LOCATIONS

System		Integrator Gain (K_i)		
Pole location	Gain (K_{open})	ξ =1.2	ξ =1.0	ξ =0.707
1	14.902	2.359	3.122	5.113
0.5	61.690	0.363	0.490	0.831
0.1	408.774	0.013	0.018	0.038

As the poles come closer to origin, the bandwidth becomes narrow, the open loop gain for the system is high and the integral gain is lower compared to that with a remote

pole location in *s*-plane.

The transient response of FLL and model at $a = 1$ for different damping conditions are illustrated in Fig. 15. Also the frequency response of the system along with the model for various pole locations at critically damped condition is shown in Fig. 16. As the poles are closer to origin the response of the system is very much sluggish. In all the cases model closely follows the system.

The transient response for different values of pole locations such as $a = 0.1$, 0.5 and 1 with different damping factors such as over-damped ($\xi = 1.2$), critically damped ($\xi = 1$) and under-damped ($\xi = 0.707$) system are shown in Fig. 17. Table II and Table III show the values of settling time for 2% tolerance (± 0.1 Hz for change of 5 Hz) of the system response for different values of damping and pole locations corresponding to change in frequency from 52.5 Hz to 47.5 Hz and vice versa respectively.

A narrow bandwidth results when the poles are closer to unit circle in *z*-plane, for the composite observer, making it sluggish. However, the bandwidth increases when the poles are far deep into the unit circle, resulting in faster response.

TABLE II. EFFECT OF POLE LOCATION AND DAMPING ON SETTLING TIME FOR FREQUENCY CHANGE FROM 52.5 - 47.5 Hz

Pole Location (a)	Settling Time		
	ξ =1.2	ξ =1.0	ξ =0.707
1.0	0.0788	0.0487	0.0557
0.5	0.1309	0.0804	0.0796
0.1	0.6319	0.4026	0.2767

TABLE III. EFFECT OF POLE LOCATION AND DAMPING ON SETTLING TIME FOR FREQUENCY CHANGE FROM 47.5 - 52.5 Hz

Pole Location (a)	Settling Time		
	ξ =1.2	ξ =1.0	ξ =0.707
1.0	0.0778	0.0452	0.0537
0.5	0.1309	0.0777	0.0779
0.1	0.6341	0.4005	0.2696

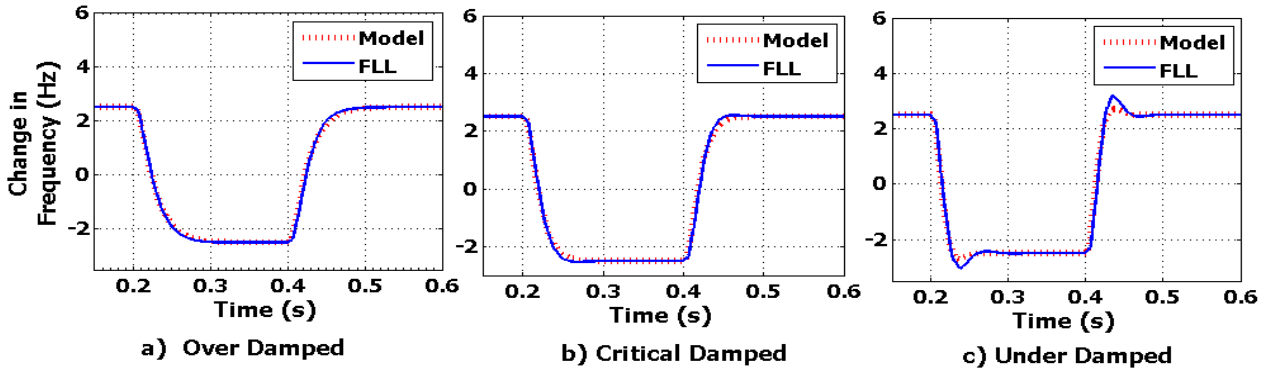

Figure 15. Transient response of proposed FLL and model for over damped, critically damped and under damped respectively with pole location corresponding to $a = 1$ for a step change in frequency from 52.5 Hz to 47.5 Hz and reinstated to 52.5 Hz at $t = 0.4$ s.

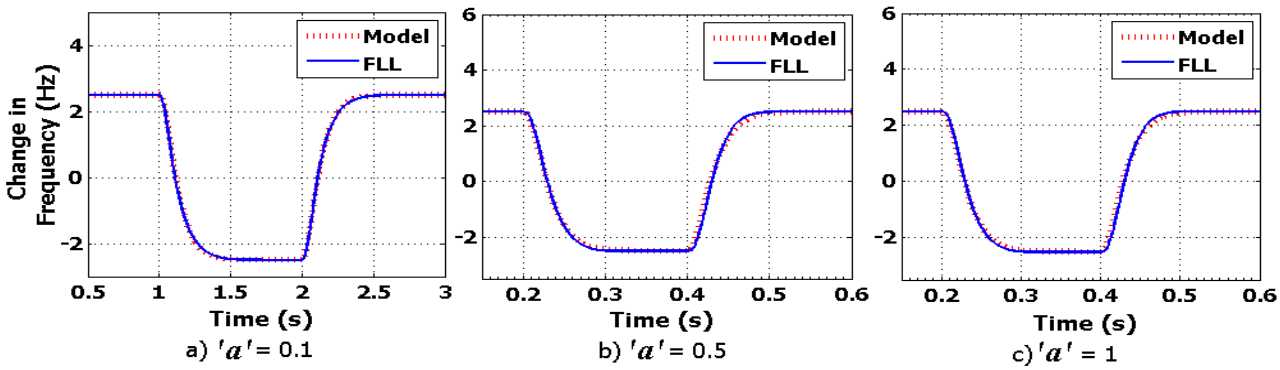

Figure 16. Transient response of proposed FLL for critically damped with various pole locations corresponding to $a = 0.1$, 0.5 and 1 respectively for a step change in frequency from 52.5 Hz to 47.5 Hz and reinstated to 52.5 Hz at $t = 0.4$ s.

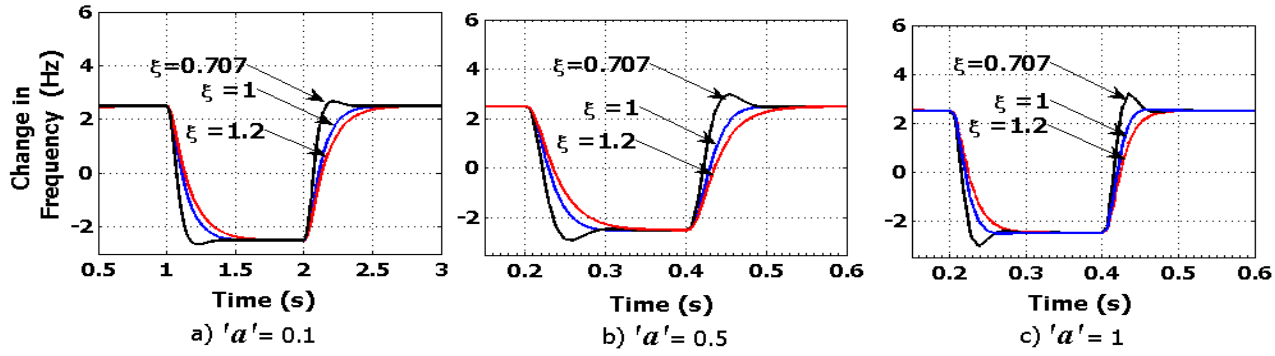

Figure 17. Transient response of FLL for under damped, critically damped and over damped with various pole location such as $a = 0.1$, 0.5 and 1, respectively for a step change frequency from 52.5 Hz to 47.5 Hz and reinstated to 52.5 Hz at $t = 0.4$ s.

V. Validation Of Proposed FLL

Simulation and experimental studies are done for the proposed observer based variable sampling frequency locked loop (FLL). The performance of the FLL is evaluated by applying a step change in frequency, phase, magnitude and DC offset for a test signal of THD 52.9 %. The pole location of the composite observer is chosen to be on a circle of radius $z = e^{-a\omega T}$, where $a = 1$, in the z-plane. Similar pole location had been chosen for the even order observer (DC and second harmonic blocks) used as filter. The integrator gain (K_i) is chosen as 3.277.

A. Step change in frequency

This harmonic rich test signal at frequency 47.5 Hz is fed to the FLL and at 0.2 s the frequency is changed to 52.5 Hz. The estimated fundamental signal, its magnitude and frequency are illustrated by simulation and experiment through Fig. 18 (a) and Fig. 18 (b) respectively. The estimation time is found to be 2.2 cycles for frequency change from 47.5 Hz to 52.5 Hz and 2.4 cycles for frequency change from 52.5 Hz to 47.5 Hz with a tolerance of 2 %.

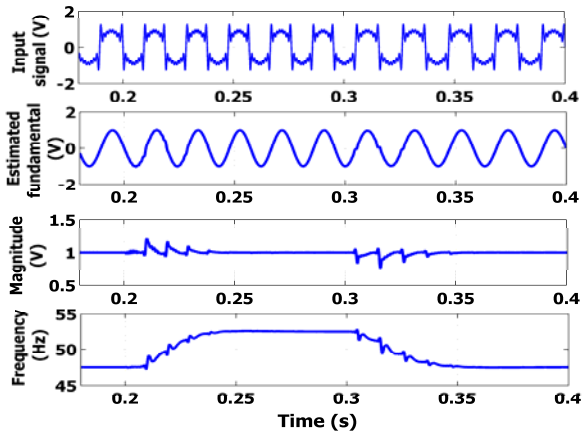

Figure 18(a). Simulation results for estimated magnitude, frequency and phase error from FLL along with the input signal for a frequency change from 47.5 Hz to 52.5 Hz at $t = 0.2$ s and reinstated to 52.5 Hz at $t = 0.4$ s.

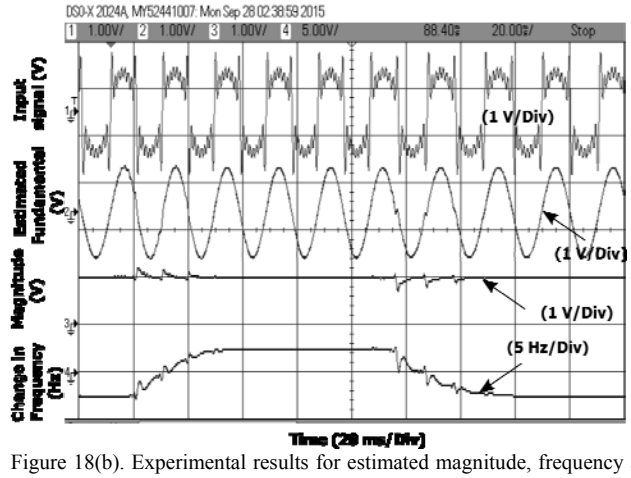

Figure 18(b). Experimental results for estimated magnitude, frequency and phase error from FLL along with the input signal for a frequency change from 47.5 Hz to 52.5 Hz at $t = 0.2$ s and reinstated to 52.5 Hz at $t = 0.4$ s.

B. Step change in Phase angle

The test signal of frequency 50 Hz is fed to the FLL and a phase jump of 40° is introduced at 0.2 s. Simulation and experimental results of the estimated fundamental signal, its magnitude and frequency along with the test signal are shown in Fig. 19 (a) and Fig. 19 (b) respectively. Even in presence of harmonics, the frequency overshoot is 4.5 Hz. The estimation of frequency is completed in 3.2 cycles.

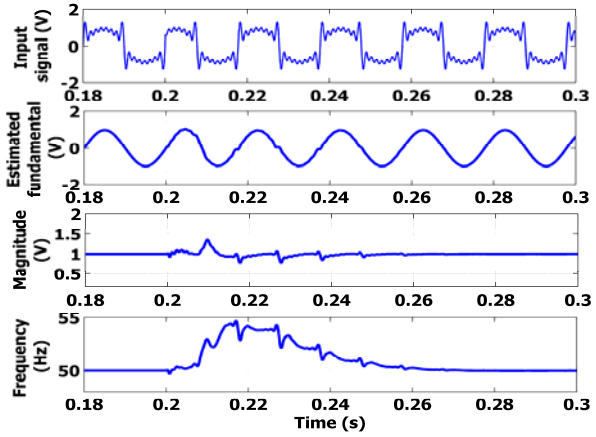

Figure 19(a). Simulation results for estimated magnitude, frequency and phase error from FLL along with the input signal for a 40° phase jump.

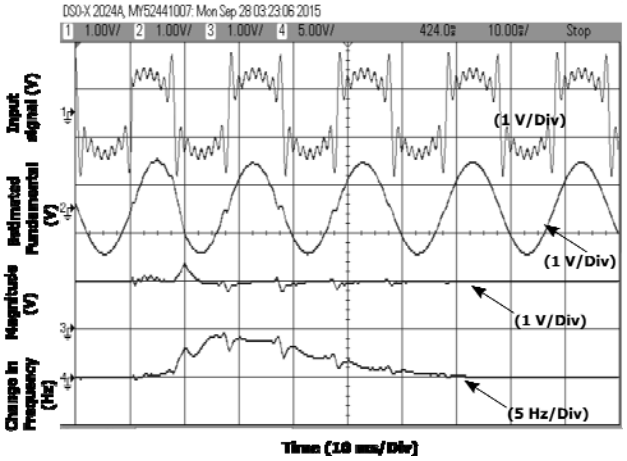

Figure 19(b). Experimental results for estimated magnitude, frequency and phase error from FLL along with the input signal for a 40° phase jump.

C. Step change in Magnitude

The test signal of frequency 50 Hz and unity magnitude is fed to the FLL. At 0.2 s, the magnitude of the signal is reduced to 60 % and reinstated after 5 cycles. Simulation and experimental results are shown in Fig. 20 (a) and

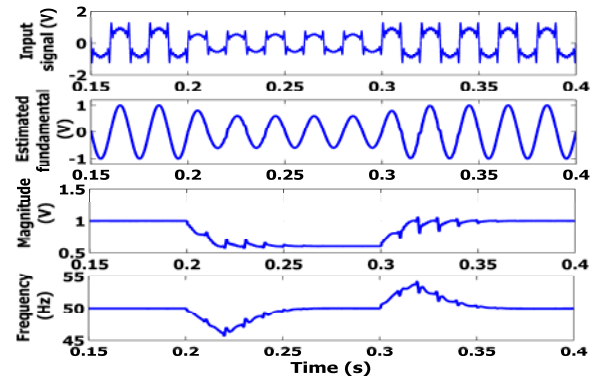

Figure 20(a). Simulation results for estimated magnitude, frequency and phase error from FLL along with the input signal for a 40 % sag in voltage which is reinstated in 5 cycles.

Fig. 20 (b) respectively to validate the estimated fundamental signal, its magnitude and frequency of the test signal. The estimation of frequency is completed in about 3 cycles.

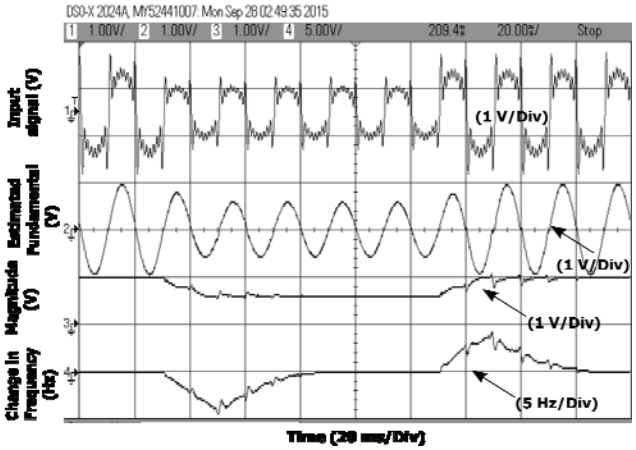

Figure 20(b). Experimental results for estimated magnitude, frequency and phase error from FLL along with the input signal for a 40 % sag in voltage which is reinstated in 5 cycles.

D. *Step change in DC offset*

A DC offset of 0.5 V is given to the test signal at 0.2 s and tested the performance of FLL. Simulation and experimental results are shown in Fig. 21 (a) and (b) which show that the FLL estimates frequency accurately, within 2.7 cycles.

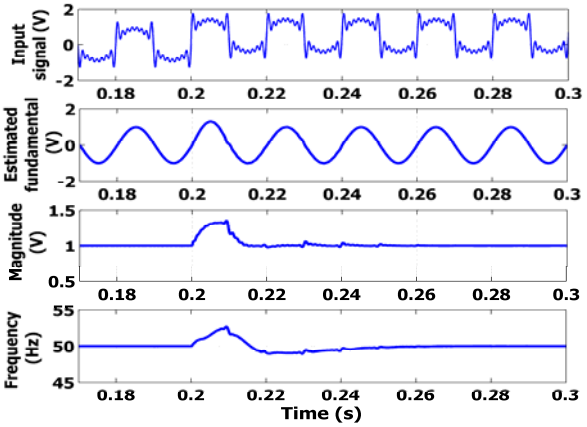

Figure 21(a). Simulation results for estimated magnitude, frequency and phase error from FLL along with the input signal with sudden DC offset of 0.5 V.

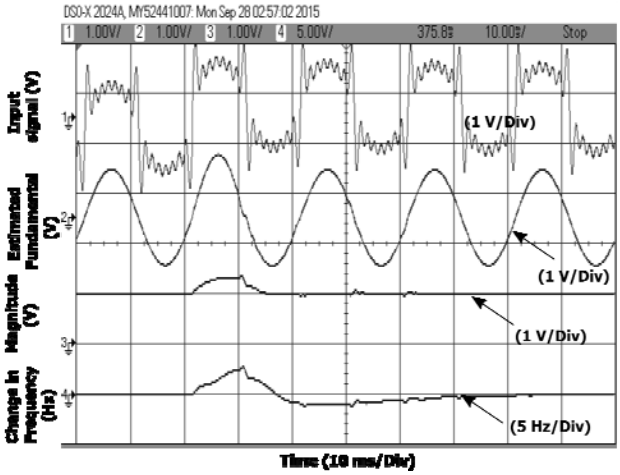

Figure 21(b). Experimental results for estimated magnitude, frequency and phase error from FLL along with the input signal with sudden DC offset of 0.5 V.

VI. APPLICATION

To illustrate the performance of the FLL, estimation of individual harmonics from a grid connected nonlinear load is considered. Further, the closed loop control of grid connected inverter using DSP builder in cyclone IV FPGA is being presented.

A. *Estimation of individual harmonics*

A rectifier type nonlinear load having a resistance of R = 36 Ω parallel with a capacitance C = 2200 μF is connected to the grid through a series inductance of 4 mH. Grid current is fed to composite observer consisting of DC and odd harmonic blocks up to the 15th. The enable signal for composite observer is derived from grid voltage through the FLL for the frequency estimation. The estimated individual harmonic components fundamental, third, fifth ….. up to the thirteenth are shown in Fig. 22 and Fig. 23 from the load current.

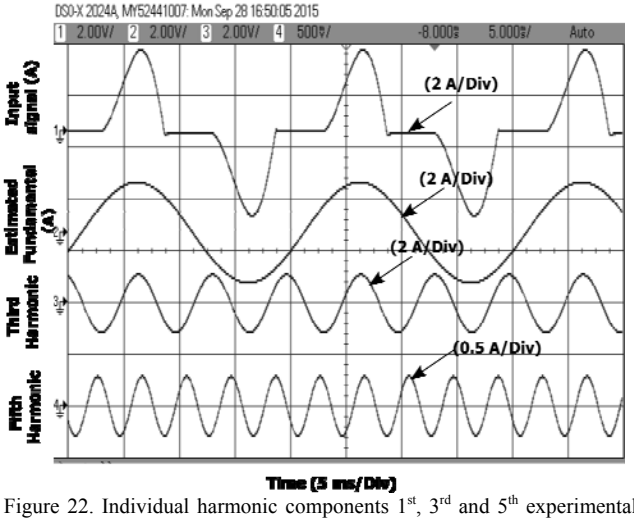

Figure 22. Individual harmonic components 1st, 3rd and 5th experimentally estimated by the FLL along with the nonlinear grid current.

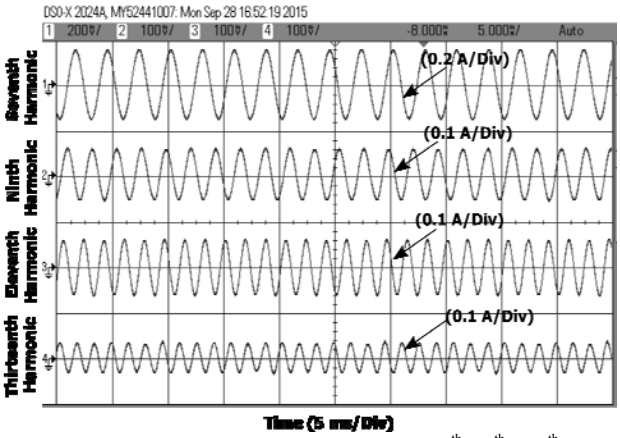

Figure 23. Individual harmonic components 7th, 9th, 11th and 13th experimentally estimated by the FLL along with the nonlinear grid current.

B. *Grid connected inverter*

To validate the performance of the scheme, the current control of grid connected inverter is implemented using variable sampling resonant controller as shown in Fig. 24. Here the grid current is regulated so as to inject power into the grid by the inverter. The proposed FLL generates the in-phase and quadrature components of the fundamental grid voltage along with the enable signal. Also a reference current of 4 A is generated in synchronism with grid voltage

from V_α and V_β with the help of FLL. I_{ref}* is calculated by $I_{ref}^{*} = I_{ref}\frac{V_\alpha}{\sqrt{(V_\alpha^2 + V_\beta^2)}}$. Error in grid current is processed through a proportional plus resonant controller to generate the control signal for PWM.

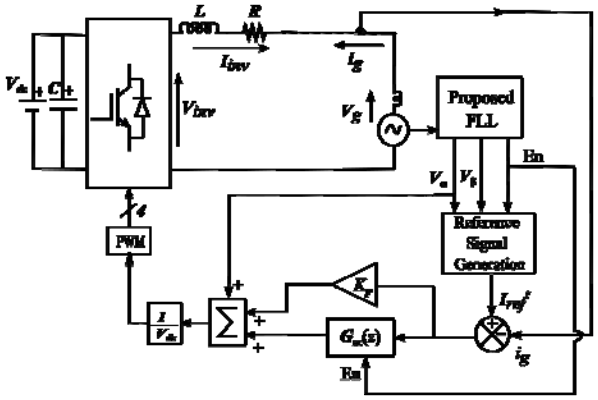

Figure 24. Block diagram of grid connected inverter.

From Fig. 24, inverter output voltage is:

$$V_{inv} = V_g + Ri_g + L\frac{di_g}{dt} \quad (28)$$

where, V_g = grid voltage, i_g = grid current, R = resistance, and L = inductance of the filter. The discrete transfer function of the Grid connected inverter is:

$$G_{inv}(z) = \frac{T/L}{z - 1 + RT/L} = \frac{g}{z - 1 + Rg} \quad (29)$$

where,

$T = \frac{0.02}{512}$, L = 4 mH, R = 0.1 Ω and $\frac{T}{L} = g = 9.7656e^{-3}$.

The transfer function model for the 'variable sampling proportional plus resonant controller' is:

$$G_c(z) = K_p + G_{rc}(z) = K_p + \frac{L_1(z - \alpha) + L_2(\alpha - 1)}{z^2 - 2\alpha z + 1} \quad (30)$$

where, 'α' is cos (ωT). The closed loop pole location of the grid connected inverter with controller is obtained as:

$$(z - 0.999)(z^2 - 2\alpha z + 1) + g(K_p z^2 + (L_1 - 2\alpha K_p)z + C) = 0 \quad (31)$$

where, $C = K_p + L_2(\alpha - 1) - L_1\alpha$.

The controller gains K_p, L_1 and L_2 are calculated using the pole placement technique. It is assumed that the desired closed loop pole locations are as per the following characteristic equation:

$$(z - h)(z^2 - 2e^{-a_c\omega T}\alpha z + e^{-2a_c\omega T}) = 0 \quad (32)$$

Comparing the coefficients of (31) and (32), the values of K_p, L_1 and L_2 are calculated as follows:

$$K_p = \frac{1}{g}(-h - 2e^{-a_c\omega T}\alpha + 0.999 + 2\alpha) \quad (33)$$

$$L_1 = \frac{1}{g}(e^{-2a_c\omega T} + 2e^{-a_c\omega T}\alpha h - 1 - 1.998\alpha + 2\alpha K_p g) \quad (34)$$

$$L_2 = \frac{1}{(\alpha - 1)g}(L_1 g\alpha + 0.999 - he^{-2a_c\omega T} - gK_p) \quad (35)$$

The bandwidth and speed of the controller are determined by the value of 'a_c' and 'h'. For this study a_c = 0.3 and h = 0.7, value of K_p = 31.37, L_1 = 0.2270 and L_2 = -3.5515.

Table IV shows the system parameter used for experimental study. The control scheme is implemented using FPGA. Fig. 25 shows the grid voltage and current when the inverter is supplying power to the grid, validating the performance of this variable sampling observer based FLL.

TABLE IV: SYSTEM PARAMETERS

Parameter	Values
DC Voltage (V_{dc})	64 V
Grid Voltage (V_g)	100 V_{p-p}
Frequency (f)	50 Hz
Filter Inductor (L)	4 mH

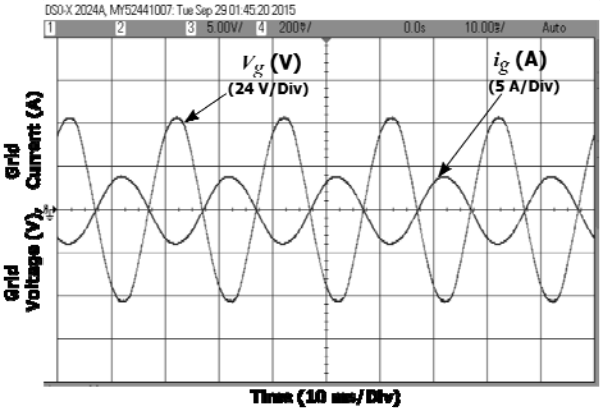

Figure 25. Grid voltage and Grid current when the inverter is injecting active power.

VII. Conclusion

In this paper, variable sampling composite observer based FLL is discussed. Whenever there is a drift in frequency, error is processed through FLL and variable sampling period pulses are generated to trigger periodically the composite observer blocks to maintain constant samples over the fundamental period. This eliminates the trigonometric computation in individual blocks of the observer making it suitable for power quality applications. The 'even harmonic' observer in feedback helps in smoother estimation of frequency. A simple design procedure is discussed to compute the integral gain corresponding to various pole locations. The performance of the variable sampling FLL is studied under different dynamic conditions such as step change in frequency, magnitude and phase angle in presence of harmonics. Real-time implementation of this FLL for individual harmonics extraction and grid connected system are also discussed. The controller designed using pole placement for grid synchronization assures stability. Implementation of these applications validates the suitability of this scheme in power quality studies and control.

References

[1] Guan-Chyun Hsieh, J. C. Hung, "Phase Locked Loop Techniques. A Survey", IEEE Transactions on Industrial Electronics, vol. 43, no. 6, pp. 609-615, 1996. doi:10.1109/41.544547

[2] T. Thacker, D. Boroyevich, R. Burgos, F. Wang, "Phase Locked Loop Noise Reduction via Phase Detector Implementation for Single Phase Systems", IEEE Transactions on Industrial Electronics, vol. 58, no. 6, pp. 2482-2490, 2011. doi:10.1109/TIE.2010.2069070

[3] S. M. Silva, B. M. Lopes, B. J. C. Filho, R. P. Campana, W. C. Bosventura, "Performance Evaluation of PLL Algorithms for Single Phase Grid Connected Systems", 39th IAS Annual Meeting of IEEE Industry Applications Society, Seattle, vol. 4, pp. 2259-2263, 2004. doi:10.1109/IAS.2004.1348790

[4] C. Subramanian, R. Kanagaraj, "Single Phase Grid Voltage Attributes Tracking for the Control of Grid Power Converters", IEEE Journal of Emerging and Selected Topics in Power Electronics, vol. 2, no. 4, pp. 1041-1048, 2014. doi:10.1109/JESTPE.2014.2341045

[5] R. M. Santos Filho, P. F. Seixas, P. C. Cortizo, L. A. B. Torres, A. F. Souza, "Comparison of Three Single Phase PLL Algorithms for UPS Applications", IEEE Transactions on Industrial Electronics, vol. 55, no. 8, pp. 2923-2932, 2008. doi:10.1109/TIE.2008.924205

[6] M. Ciobotaru, R. Teodorescu, F. Blaabjerg, "A New Single Phase PLL Structure based on Second Order Generalized Integrator", 37th IEEE Power Electronics Specialists Conference PESC, Jeju, pp. 1-6, 2006. doi:10.1109/pesc.2006.1711988

[7] S. Golestan, M. Monfared, F. D. Freijedo, J. M. Guerrero, "Dynamics Assessment of Advanced Single Phase PLL Structures", IEEE Transactions on Industrial Electronics, vol. 60, no. 6, pp. 2167-2177, 2013. doi:10.1109/TIE.2012.2193863

[8] K. De Brabandere, T. Loix, K. Engelen, B. Bolsens, J. Van den Keybus, J. Driesen, R. Belmans, "Design and Operation of a Phase Locked Loop with Kalman Estimator-based Filter for Single Phase Applications", 32nd Annual Conference on the IEEE Industrial Electronics Society IECON, Paris, pp. 525-530, 2006. doi:10.1109/IECON.2006.348099

[9] M. Karimi-Ghartemani, M. R. Iravani, "A Method for Synchronization of Power Electronic Converters in Polluted and Variable Frequency Environments", IEEE Transactions on Power Systems, vol. 19, no. 3, pp. 1263-1270, 2004. doi:10.1109/TPWRS.2004.831280

[10] M. Karimi-Ghartemani, "A Unifying Approach to Single Phase Synchronous Reference Frame PLLs", IEEE Transaction on Power Electronics, vol. 28, no. 10, pp. 4550-4556, 2013. doi:10.1109/TPEL.2012.2235185

[11] M. Karimi-Ghartemani, "A Distortion-free Phase Locked Loop system for FACTS and Power Electronic Controllers", International Journal of Electric Power System Research, Elsevier, vol. 77, no. 8, pp. 1095-1100, 2007. doi:10.1016/j.epsr.2006.09.013

[12] M. Karimi-Ghartemani, S. A. Khajehoddin, P. K. Jain, A. Bakhshai, M. Mojiri, "Addressing DC Component in PLL and Notch Filter Algorithms", IEEE Transactions on Power Electronics, vol. 27, no. 1, pp. 78-86, 2012. doi:10.1109/TPEL.2011.2158238

[13] Fengjiang Wu, Dongyang Sun, Lujie Zhang, Jiandong Duan, "Influence of Plugging DC offset Estimation Integrator in Single Phase EPLL and Alternative Scheme to Eliminate Effect of Input DC Offset and Harmonics", IEEE Transactions on Industrial Electronics, vol. 62, no. 8, pp. 4823-4831, 2015. doi:10.1109/TIE.2015.2405496

[14] M. Karimi-Ghartemani, "Linear and Pseudo-linear Enhanced Phase Locked Loop (EPLL) Structures", IEEE Transactions on Industrial Electronics, vol. 61, no. 3, pp. 1464-1474, 2014. doi:10.1109/TIE.2013.2261035

[15] I. Carugati, P. Donato, S. Maestri, D. Carrica, M. Benedetti, "Frequency Adaptive PLL for Polluted Single Phase Grids", IEEE Transactions on Power Electronics, vol. 27, no. 5, pp. 2396-2404, 2012. doi:10.1109/TPEL.2011.2172000

[16] C. M. Orallo, I. Carugati, S. Maestri, P. G. Donato, D. Carrica, M. Benedetti, "Harmonics Measurement with a Modulated Sliding Discrete Fourier Transform Algorithm", IEEE Transactions on Instrumentation and Measurement, vol. 63, no. 4, pp. 781-793, 2014. doi:10.1109/TIM.2013.2287801

[17] K. Arun, K. Selvajyothi, "Cascaded Delayed Signal Cancellation based Variable Sampling SRF PLL", Mediterranean Journal of Measurement and Control, vol. 12, no. 1, pp. 511-520, 2016.

[18] D. Yazdani, A. Bakhshai, G. Joos, M. Mojiri, "A Real-time Extraction of Harmonic and Reactive Current in a Nonlinear Load for Grid Connected Converters", IEEE Transactions on Industrial Electronics, vol. 56, no. 6, pp. 2185-2189, 2009. doi:10.1109/TIE.2009.2017100

[19] M. Mojiri, M. Karimi-Ghartemani, A. Bakhshai, "Estimation of Power System Frequency using an Adaptive Notch Filter", IEEE Transactions on Instrumentation and Measurement, vol. 56, no. 6, pp. 2470-2477, 2007. doi:10.1109/TIM.2007.908631

[20] M. Mojiri, M. Karimi-Ghartemani, A. Bakhshai, "Time-domain Signal Analysis using Adaptive Notch Filter", IEEE Transactions on Signal Processing, vol. 55, no. 1, pp. 85-93, 2007. doi:10.1109/TSP.2006.885686

[21] P. Rodriguez, A. Luna, I. Candela, R. Teodorescu, F. Blaabjerg, "Grid Synchronization of Power Converters using Multiple Second Order Generalized Integrators", 34th Annual Conference on IEEE Industrial Electronics Society IECON, Orlando, Florida, pp. 755-760, 2008. doi:10.1109/IECON.2008.4758048

[22] P. Rodriguez, A. Luna, I. Candela, R. Mujal, R. Teodorescu, F. Blaabjerg, "Multiresonant Frequency Locked Loop for Grid Synchronization of Power Converters under Distorted Grid Conditions", IEEE Transactions on Industrial Electronics, vol. 58, no. 1, pp. 127-138, 2011. doi:10.1109/TIE.2010.2042420

[23] K. Selvajyothi, P. A. Janakiraman, "Extraction of Harmonics using Composite Observers", IEEE Transactions on Power Delivery, vol. 23, no. 1, pp. 31-40, 2008. doi:10.1109/TPWRD.2007.911141

[24] R. Costa-Castello, R. Grino, E. Fossas, "Odd-harmonic Digital Repetitive Control of a Single Phase Current Active filters", IEEE Transactions on Power Electronics, vol. 19, no. 4, pp. 1060-1068, 2004. doi:10.1109/TPEL.2004.830045

[25] Zhi-Xiang Zou, Keliang Zhou, Zheng Wang, Ming Cheng, "Frequency-adaptive Fractional-order Repetitive Control of Shunt Active Power Filters", IEEE Transactions on Industrial Electronics, vol. 62, no. 3, pp. 1659-1668, 2015. doi:10.1109/TIE.2014.2363442

[26] C. S. Turner, "Recursive Discrete-time Sinusoidal Oscillators", IEEE Signal Processing Magazine, vol. 20, no. 3, pp. 103-111, 2003. doi:10.1109/MSP.2003.1203213